Kinetic Characterization of the Weak Binding States of Myosin V†

Christopher M. Yengo,‡ Enrique M. De La Cruz,§ Daniel Safer, E. Michael Ostap, and H. Lee Sweeney*

University of Pennsylvania School of Medicine, Department of Physiology and Pennsylvania Muscle Institute, Philadelphia, Pennsylvania 19104

Received November 26, 2001; Revised Manuscript Received April 5, 2002

ABSTRACT: Myosin V is a molecular motor shown to move processively along actin filaments. We investigated the properties of the weak binding states of monomeric myosin V containing a single IQ domain (MV 1IQ) to determine if the affinities of these states are increased as compared to conventional myosin. Further, using a combination of non-hydrolyzable nucleotide analogues and mutations that block ATP hydrolysis, we sought to probe the states that are populated during ATP-induced dissociation of actomyosin. MV 1IQ binds actin with a $K_d = 4$ μM in the presence of ATPγS at 50 mM KCl, which is 10−20-fold tighter than that of nonprocessive class II myosins. Mutations within the switch II region trapped MV 1IQ in two distinct M.ATP states with very different actin binding affinities ($K_d = 0.2$ and 2 μM). Actin binding may change the conformation of the switch II region, suggesting that elements of the nucleotide binding pocket will be in a different conformation when bound to actin than is seen in any of the myosin crystal structures to date.

Myosin V is an actin-based motor protein that is capable of moving processively along actin (*1*−*3*) (i.e., proceeding through more than one catalytic cycle per encounter with actin). Since myosin V and myosin VI are the first myosins suggested to move processively, similar to members of the kinesin family of motor proteins, it is of interest to determine what enzymatic and kinetic features lead to their processive behavior.

Initial characterizations of myosin V noted that it remained bound to actin in the presence of ATP (*4*). This led to speculation that the M.ATP and M.ADP.Pi states of myosin V might have much higher actin affinities than the corresponding states of myosin II. However, delineation of most of the kinetic steps (Scheme 1) in the ATPase pathway of monomeric myosin V (*5*−*9*) revealed that myosin V primarily populates an ADP state in the presence of actin and ATP. Myosin V binds ATP similarly to myosin II, but it hydrolyzes ATP extremely fast in the absence of actin (k_{+3}), and it binds to actin (k_{+9}) and rapidly releases phosphate (k_{+4}') in the posthydrolysis AM.ADP.Pi state, which results in a rate-limiting ADP-release (k_{+5}') step.

Thus, myosin V has a higher duty ratio (i.e., fraction of ATPase cycle myosin is strongly bound to actin) than myosin II, which allows it to have a higher affinity for actin in the presence of ATP (*5*−*8*). However, whether the normally weak binding states (AM.ATP and AM.ADP.Pi) have a greater affinity for actin than the corresponding states of myosin II is an open question.

Scheme 1

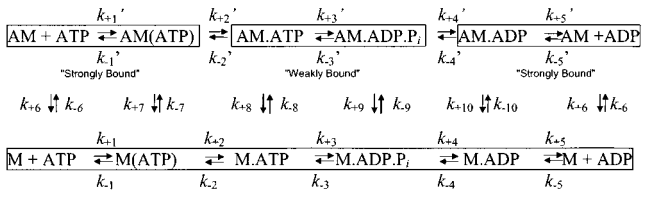

Although the actin affinity of different myosin isoforms may vary, the coupling that occurs between the nucleotide- and actin-binding regions may be well conserved. Crystallographic studies have determined that myosin contains a conserved structural core that includes the switch I and II regions, which coordinate the nucleotide in a manner similar to kinesin and G-proteins (reviewed in *10*). The conformation of the switch II region appears to directly affect the position of the light chain binding region, which is thought to function as a lever arm during force generation (*11*). In contrast, the switch I region has not been found to change conformation in the structures studied thus far. However, it is unclear whether the switch I and II regions may also play a role in altering the conformation of the actin-binding region in a nucleotide-dependent manner.

To investigate the weakly bound states and examine the coupling between the nucleotide- and actin-binding regions of myosin V, we have used two different strategies. First we have used non-hydrolyzable ATP analogues (ATPγS and AMPPNP) to trap myosin V in the prehydrolysis ATP states. These analogues are of particular interest in light of the fact that high-resolution structures of myosin II with either analogue bound at the active site are essentially the same (*12*), while the corresponding affinities of myosin for actin are quite different (*13*−*15*). Second, we made single-point

† This work was supported by National Institute of Health Grant AR35661 (to H.L.S.).

* Corresponding author. Address: Department of Physiology, A700 Richards Bldg., University of Pennsylvania School of Medicine, Philadelphia, PA 19104-6085. Tel.: 215-898-0486. Fax: 215-898-0475. E-mail: Lsweeney@mail.med.upenn.edu.

‡ A National Institute of Health, NRSA Postdoctoral Fellow.

§ A Burroughs Wellcome Fund Fellow of the Life Sciences Research Fundation. Current address: Yale University, Department of Molecular Biophysics & Biochemistry, 423A J.W. Gibbs, 266 Whitney Avenue, New Haven, CT 06520.

10.1021/bi015969u CCC: $22.00
Published on Web 06/05/2002

mutations in the switch II region of myosin V, G440A and E442A, that were shown to inhibit the hydrolysis of ATP in studies of *Dictylostelium* and smooth muscle myosin II (*16*−*19*). The G440A mutant eliminates a highly conserved hydrogen bound to the γ phosphate of ATP, whereas the E442A mutant disrupts the coordination of the water molecule involved in the hydrolysis of ATP and eliminates a highly conserved salt bridge.

These two methods have allowed us to delineate a number of weakly bound states of myosin V and provide new insights into the coupling between the nucleotide- and actin-binding regions of myosin. In addition, our results allow us to speculate on the role that the weak binding states play in the mechanism of myosin V processivity.

EXPERIMENTAL PROCEDURES

Reagents. All reagents were the highest purity commercially available. ATP was prepared fresh from powder (Roche Molecular Biochemicals, 99.7% pure by HPLC[1]; data not shown). ATPγS[1] and AMPPNP[1] (Roche Molecular Biochemicals) were purified by ion-exchange chromotography (purity, >98%). *N*-Methylanthraniloyl (mant)[1] labeled ADP and ATP were prepared as described (*20*), and mant labeled AMPPNP was obtained from Molecular Probes. ATP and ADP concentrations were determined by absorbance at 259 nm using ϵ_{259} of 15 400 M^{-1} cm^{-1}. Nucleotides were prepared prior to use in the presence of equimolar $MgCl_2$.

Myosin V cDNA Construction, Expression, and Purification. Site-directed mutagenesis was performed on a construct of chicken myosin V containing a single IQ motif (WT MV 1IQ) (residues 1−792) to substitute glycine 440 (G440A MV 1IQ) or glutamate 442 (E442A MV 1IQ) with alanine. The baculovirus system was used to express mutant and wild-type chicken myosin V which contained a C-terminal FLAG tag for purification purposes (*5*). All myosin V constructs were coexpressed with the essential light chain LC-1sa (*7*) and purified using an anti-FLAG affinity chromotography. The purity was greater than 95% based on Coomassie stained SDS gels.

Actin was purified from rabbit skeletal muscle using an acetone powder method (*21*) and gel filtered. Actin was labeled with pyrene iodoacetamide (Molecular Probes) (*22*) when necessary.

Steady-State ATPase Activity of MV 1IQ. All assays were performed in KMg50 buffer (50 mM KCl, 1 mM EGTA, 1 mM $MgCl_2$, 1 mM DTT, and 10 mM imidozole−HCl pH 7.0, 25 °C). Steady-state ATP hydrolysis by MV 1IQ LC-1sa (50−100 nM) was examined using the NADH-linked assay (*6*), with a final MgATP concentration of 1 mM. ATPγS hydrolysis was examined by measuring the time course of ADP production using HPLC (final concentrations, MV1IQ = 0.2−1.0 μM and ATPγS = 0.5−1 mM).

Determination of ADP−Pi Burst. The amplitude of the ADP−Pi burst of MV 1IQ was determined in KMg50 buffer at 25 °C using an activated charcoal extraction method to measure the ^{32}Pi generated from the hydrolysis of [γ-^{32}P]-ATP as described (*23*). The final concentrations were 2.5 μM MV 1IQ and 100μM ATP.

Intrinsic Tryptophan Fluorescence Measurements of MV 1IQ. Steady-state tryptophan fluorescence of WT and mutant MV 1IQ was measured in KMg50 at ∼20 °C with an Alphascan fluorimeter (Photon Technology International, Alpha Scan, Brunwick, NJ). A sample of 1μM MV 1IQ was excited with a wavelength of 295 nm and the fluorescence emission spectrum scanned from 300−400 nm. The fluorescence emission spectrum was corrected for background fluorescence and dilution effects.

Stopped-Flow Measurements and Kinetic Modeling. Transient kinetic experiments were performed in a Applied Photophysics (Surrey, UK) stopped-flow with a dead-time of 1.2 ms. Tryptophan fluorescence was measured by exciting the sample at 295 nm and the emission measured using a 320 nm long pass filter (Oriel Corp., Stratford, CT). Pyrene actin was excited at 365 nm, and mant-labeled nucleotides were excited by energy transfer at 295 nm or directly at 365 nm; the fluorescence emission of both pyrene and mant was measured using a 400 nm long pass filter (Oriel Corp., Stratford, CT).

Nonlinear least-squares fitting of the data was done with software provided with the instrument or Kaleidagraph (Synergy Software, Reading, PA). Uncertainties reported are standard error of the fits unless stated otherwise.

Actin Co-Sedimentation Assays. MV 1IQ (1μM) was equilibrated with a range of actin concentrations (0−80 μM) for 30 min on ice. Samples of 3−4 mM ATPγS, 5−15 mM AMPPNP, or 1 mM ATP were added just prior to ultracentrifugation at 4 °C in a TLA 120.1 Beckman or at 95 000 rpm for 30 min. Samples were prepared as stated above for measurements performed at 25 °C, except the samples were incubated for 10 min at 25 °C prior to ultracentrifugation at 25 °C. The amount of actin-bound myosin was determined by comparing the amount of MV 1IQ heavy chain in the supernatant, normalized to the absence of actin, using scanned Coomassie stained SDS gels or HPLC analysis, yielding essentially the same results. The amount of contaminating ADP in the supernatant was determined by HPLC, which was only significant in the experiments with ATPγS (≤2% at 4 °C and ≤10% at 25 °C), and the data were corrected for the amount of AM.ADP using the competitive binding equilibrium equation: $[AM.ADP]/[AM.ATP\gamma S] = ([ATP\gamma S]/K_{ATP\gamma S})/\{1 + ([ATP\gamma S]/K_{ATP\gamma S}) + ([ADP]/K_{ADP})\}$, where $K_{ATP\gamma S}$ and K_{ADP} are the affinities of ATPγS and ADP for actomyosin V. The dissociation constant for actin (K_d^{app}) was determined by fitting the data to the quadratic equation $[AM] = \{([M]_0 + [A]_0 + K_d^{app}) \pm [([M]_0 + [A]_0 + K_d^{app})^2 - 4([A]_0[M]_0)]^{0.5}\}/2$, where $[M]_0$, $[A]_0$, and [AM] are the actin, myosin, actomyosin concentrations, respectively (*24*).

RESULTS

Steady-State MV 1IQ ATPase Activity. The steady-state turnover of ATP by MV 1IQ is very slow (0.02 s^{-1}) in the absence of actin and is limited by phosphate release (k_{+4}), while actin activates the ATPase more than 500-fold (V_{MAX} ∼ 15 s^{-1}, K_{ATPase} ∼ 2 μM) and causes ADP release to be rate-limiting (*5*−*7*). MV 1IQ hydrolyzes ATPγS at a very slow rate at 4 °C (≤0.008 ± 0.001 s^{-1}), and actin does not activate the ATPase activity (Table 1). At 25 °C, MV 1IQ

[1] Abbreviations: HPLC, high-performance liquid chromatography; mantADP, *N*-methylanthraniloyl, 2′-deoxyadenosine 5′-diphosphate; mantATP, *N*-methylanthraniloyl, 2′-deoxyadenosine 5′-triphosphate; ATPγS, adenosine 5′-[γ-thio]triphosphate; AMPPNP, adenosine 5′-($\beta\gamma$-imidotriphosphate).

Table 1: Steady-State ATPase Properties of WT and Mutant MV 1IQ

MV (nucleotide)	Trp fluorescence enhancement (% increase)	Pi burst (Pi·head^{-1})	0 actin ATPase (s^{-1}·head^{-1})	10 μM actin ATPase (s^{-1}·head^{-1})
WT(ATP)	13 (±2)	0.9 (± 0.1)[a]	≤ 0.06 (± 0.001)[b]	17 (± 0.2)[b]
WT(ATPγS) 25 °C	0	n.d.	0.2 (± 0.1)[c]	0.02 (± 0.004)[c]
WT(ATPγS) 4 °C	n.d.	n.d.	≤ 0.008 (± 0.001)[c]	0.024 (± 0.004)[c]
WT(AMPPNP)	8 (±2)	n.d.	n.a.	n.a.
G440A(ATP)	0	0[a]	≤ 0.01(± 0.01)[b]	≤ 0.04 (± 0.01)[b]
E442A(ATP)	8 (±1)	0[a]	≤ 0.0001 (± 0.0)[d]	≤ 0.01 (± 0.01)[b]

[a] Rapid quench of MV [^{32}P-γ]ATP. [c] HPLC. [b] NADH coupled assay. [d] Single turnover tryptophan fluorescence.

Scheme 2

$$M + ATP \overset{K_1}{\leftrightarrow} M(ATP) \overset{K_2}{\leftrightarrow} M^*.ATP \overset{K_{3a}}{\leftrightarrow} M^{**}.ATP \overset{K_{3b}}{\leftrightarrow} M^{**}ADP.Pi \overset{K_4}{\leftrightarrow} M.^*ADP \overset{K_5}{\leftrightarrow} AM$$

hydrolyzes ATPγS at a similar or slightly faster rate than that of ATP (0.2 ± 0.1 and ≤0.06 ± 0.001 s^{-1}, respectively). The turnover of ATPγS is inhibited by actin (0.020 ± 0.004 s^{-1} at 10 μM actin) (see Table 1) in an actin-concentration-dependent manner (inhibition was 50% of maximum inhibition at ~3 μM actin, data not shown). AMPPNP was not hydrolyzed by MV 1IQ at 4 or 25 °C over a 30 min period.

The turnover of ATP by the G440A and E442A MV 1IQ mutants was extremely slow and was not activated by actin (Table 1). Neither mutant generated a Pi burst ([ADP−Pi]/[myosin]) which was found to be near 1 for WT MV 1IQ (*5*, *6*) (Table 1). The steady-state turnover of ATP measured in the NADH coupled assay was extremely slow for both the G440A and E442A MV 1IQ mutants in the absence (≤0.01 ± 0.01 s^{-1} and ≤0.05 ± 0.01 s^{-1}, respectively) and presence of actin (≤0.01 ± 0.04 s^{-1} and ≤0.01 ± 0.0 s^{-1}, respectively) (see Table 1). A single turnover of ATP hydrolysis by the E442A MV 1IQ mutant in the absence of actin monitored using the intrinsic tryptophan fluorescence signal (see section below) demonstrated the turnover of ATP by this mutant, determined at a higher resolution than the that of NADH assay, is at least 100-fold slower than that by WT MV 1IQ (≤0.0001 ± 0.000 01 s^{-1}) (Table 1).

Tryptophan Fluorescence Enhancement of MV 1IQ Nucleotide Complexes. To determine the predominant steady-state intermediates of MV 1IQ in the presence of ATP analogues and mutant MV 1IQ in the presence of ATP, we examined the intrinsic tryptophan fluorescence of MV 1IQ (Figure 1 and Table 1). Studies on myosin II have determined that the intrinsic tryptophan fluorescence signal increases upon ATP binding (M*.ATP) and increases further upon formation of the hydrolysis-competent state (M**.ATP), which precedes and limits the rate of ATP hydrolysis (see Scheme 2, where M* represents enhanced tryptophan fluorescence) (*25*, *26*).

It has been proposed that the increase in tryptophan fluorescence of myosin V monitors the formation of the hydrolysis-competent state (M**.ATP), which is the step (K_{3a}) that precedes and limits ATP hydrolysis, but does not respond to ATP binding (K_2) (*5*).

The results summarizing the nucleotide-dependent change in the tryptophan fluorescence of MV 1IQ are shown in Figure 1. The tryptophan fluorescence of WT MV 1IQ increased 12−15% in the presence of ATP, increased 8−10% in the presence of AMPPNP, and did not increase in the presence of ATPγS (Figure 1A). The intrinsic fluorescence of G440A MV 1IQ did not increase in the presence of ATP, while the intrinsic fluorescence of E442A MV 1IQ increased 7−8% (Figure 1B).

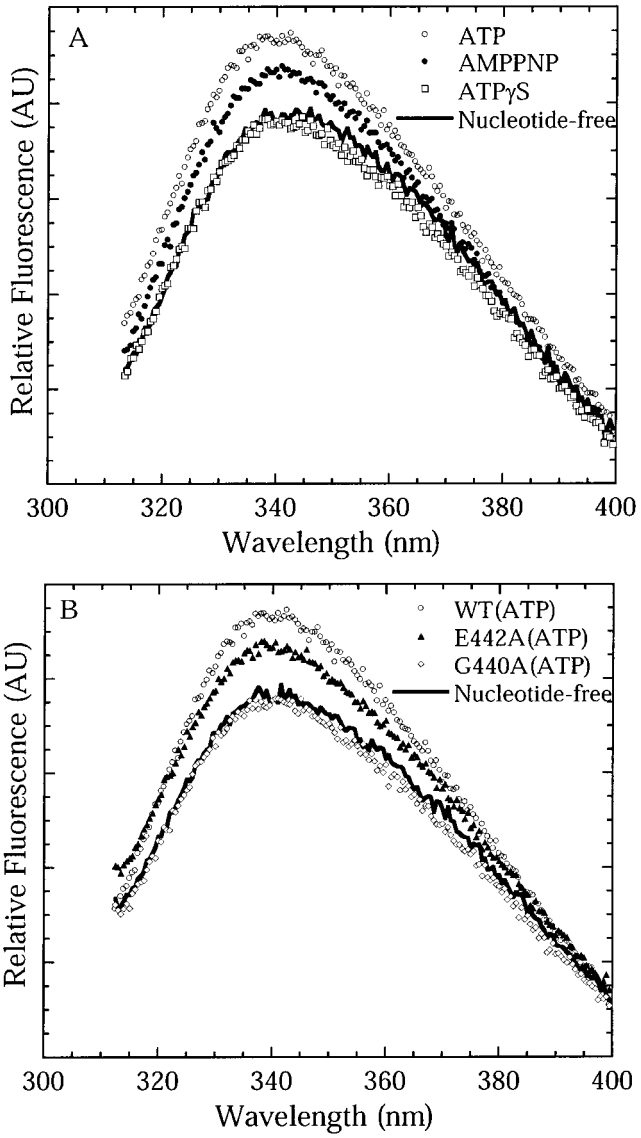

FIGURE 1: Nucleotide-dependent intrinsic tryptophan fluorescence enhancement of MV 1IQ. (A) Tryptophan fluorescence enhancement of WT MV 1IQ in the presence of ATP, ATPγS, or AMPPNP binding compared to the absence of nucleotide. (B) The tryptophan fluorescence enhancement of G440A or E442A MV 1IQ upon ATP binding compared to the nucleotide-free conditions. The fluorescence of 1 μM myosin V 1IQ in KMg50 buffer at 25 °C in the presence and absence of 100 μM ATP or ATP analogues was excited at 295 nm, and the emitted fluorescence was measured in a fluorimeter from 300 to 400 nm. The percent increase in tryptophan fluorescence intensity relative to nucleotide free conditions is summarized in Table 1.

Nucleotide Binding to MV 1IQ Monitored with Mant-Labeled Nucleotides. We measured ATPγS and AMPPNP

Table 2: Transient Kinetic Analysis of Mutant and WT MV 1IQ

MV 1IQ LC-1sa nucleotide complex	nucleotide binding to myosin K_1k_{+2} (μM^{-1} s^{-1})	nucleotide binding to actomyosin $K_1'k_{+2}'$ (μM^{-1} s^{-1})	nucleotide binding to actomyosin K_1' (μM)	dissociation from actin k_{+2}' (s^{-1})	apparent actin affinity K_d^{app}(μM)
WT (ATP)	1.4 (±0.2)[a]	1.0 (±0.1)[b]	925 (±109)	899 (±43)[b]	–
WT (ATPγS)[c]	n.d.	n.d.	n.d.	10 (±3.7)[b]	4.0 (±1.0)[d]
WT (ATPγS)	2.1 (±0.03)[e]	0.16 (±0.04)[e,b]	400 (±160)	66 (±10)[b]	13 (±2.0)[d]
WT (AMPPNP)	0.07 (±0.01)[a,e]	0.003 (±0.0001)[b]	248 (±81)	0.8 (±0.1)[b]	0.3 (±0.1)[d]
G440A (ATP)	1.3 (±0.1)[e]	0.005 (±0.001)[b] 1.2 (±0.1)[e]	398 (±71)	2.2 (±0.1)[b]	0.2 (±0.02)[d]
E442A (ATP)	2.7 (±0.6)[a]	2.3 (±0.2)[b]	387 (±40)	874 (±28)[b]	1.6 (±0.2)[d]

[a] Trp Fluorescence. [b] Pyrene Actin Fluorescence. [c] Measured at 4 °C. [d] Sedimentation Assay. [e] *Mant* Fluorescence.

binding to MV 1IQ and actomyosin V 1IQ by competition with the fluorescently labeled nucleotide, mantADP (Figure 2 and Table 2). The fluorescence of mantADP increases when bound to myosin. Therefore, we could monitor the rate of ATPγS (Figure 2A) or AMPPNP (Figure 2B) binding to MV 1IQ by its ability to compete with mantADP. The rate of nucleotide binding, k_{obs} $(sec)^{-1}$, increased linearly as a function of ATP analogue concentration and was fit to the equation k_{obs} $(sec)^{-1} = k_{mD}[mantADP] + k_{Analog}[ATP\ analog]$, assuming irreversible binding of the nucleotide to myosin (*27*), where k_{mD} and k_{Analog} are the second-order rate constants for mantADP and ATP analogue binding to MV 1IQ, respectively. The rate of mantADP binding to MV 1IQ was determined to be 5 μM^{-1} s^{-1}. The second-order rate constant for ATPγS binding to myosin V (K_1k_{+2}) was found to be 2.1 ± 0.1 μM^{-1} s^{-1}, similar to that of ATP (K_1k_{+2} = 1.4 ± 0.1 μM^{-1} s^{-1}), while AMPPNP bound at a rate 10-fold slower (K_1k_{+2} = 0.18 ± 0.10 μM^{-1} s^{-1}). The rate of mantAMPPNP binding to MV 1IQ was within 2−3-fold (K_1k_{+2} = 0.07 ± 0.01 μM^{-1} s^{-1}) of that determined with the mantADP competition method, suggesting this method is a valid for estimating the association rate constants. In addition, the linear fit of the mantAMPPNP binding data extrapolates through zero, suggesting this nucleotide analogue binds MV 1IQ essentially irreversibly and validates this assumption made in the mantADP competition method. The rate of ATPγS binding to actomyosin V 1IQ monitored with the mantADP competition method was determined to be 10−20-fold slower ($K_1'k_{+2}'$ = 0.09 ± 0.01 μM^{-1} s^{-1}) than in the absence of actin (data not shown).

The binding of ATP to G440A MV 1IQ in the presence and absence of actin, monitored by direct binding of mantATP, was found to be similar to that of WT MV 1IQ (K_1k_{+2} and $K_1'k_{+2}' \sim 1-2$ μM^{-1} s^{-1}) (Table 2).

Nucleotide Binding Monitored by Intrinsic Tryptophan Fluorescence. The maximum rate of the tryptophan fluorescence signal obtained from the plot of k_{obs} as a function of ATP concentration is thought to monitor formation of the hydrolysis-competent step with ATP ($k_{+3a} + k_{-3b}$) because $k_{+2} \gg k_{+3a}$ (see Scheme 2). In addition, the initial slope of this plot defines the second-order rate constant for ATP binding. The increase in tryptophan fluorescence observed upon AMPPNP binding to MV 1IQ was used to monitor the rate of binding of this nucleotide, which was similar (K_1k_{+2} = 0.06 ± 0.01 μM^{-1} s^{-1}) to that determined by the mantAMPPNP binding method. The maximum rate of tryptophan fluorescence signal obtained with AMPPNP (4.1 ± 0.2 s^{-1}) (Figure 3A) was 200-fold slower than that with ATP.

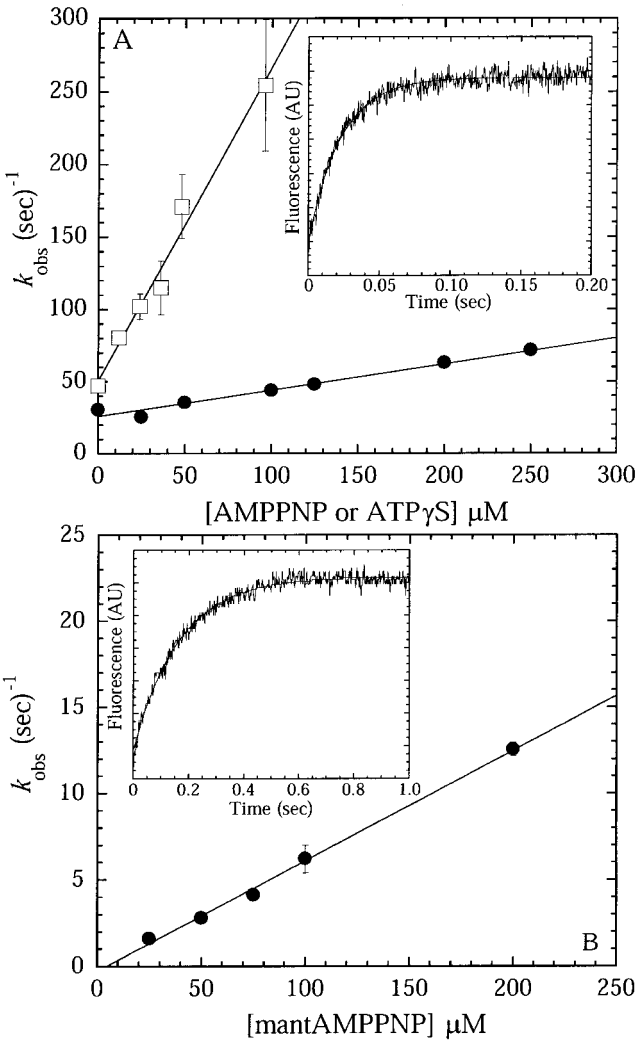

FIGURE 2: Nucleotide binding to myosin 1IQ monitored by competition with mant ADP or direct binding with mantAMPPNP. A fixed amount of mantADP (6 μM) and different concentrations of (A) ATPγS or AMPPNP were mixed with 1 μM MV 1IQ. The rate of nucleotide binding, k_{obs} $(sec)^{-1}$, increased linearly as a function of ATP analogue concentration and was fit to the equation k_{obs} $(sec)^{-1} = k_{mD}[mantADP] + k_{Analog}[ATP\ analog]$ assuming irreversible binding of the nucleotide to myosin. (Inset: Time course of fluorescence enhancement after mixing 6 μM mantADP and 100 μM AMPPNP with 0.5 μM MV 1IQ. The solid line is the best fit to a single exponential with a rate of 44.8 ± 0.9 s^{-1}.) (B) The rate of mantAMPPNP binding to MV 1IQ was measured by mixing 1 μM MV 1IQ with varying concentrations of mantAMPPNP. (Inset: Time course of fluorescence enhancement after mixing 100 μM mantAMPPNP with 1 μM MV 1IQ. The solid line is the best fit to a single exponential with a rate of 6.2 ± 0.8 s^{-1}.)

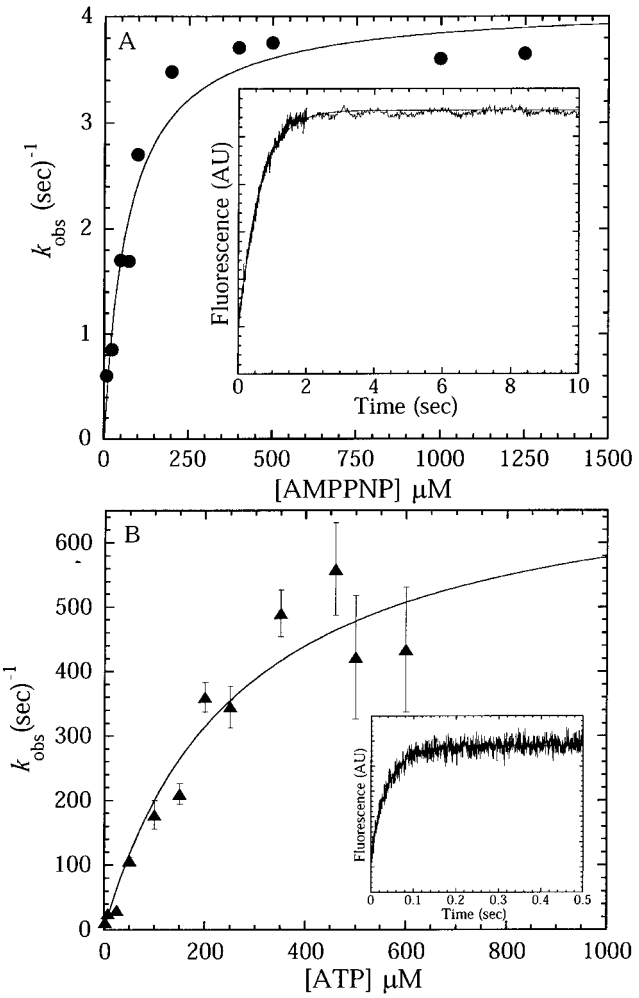

FIGURE 3: Kinetics of the nucleotide-induced increase in tryptophan fluorescence of WT and E442A MV 1IQ. Dependence of the k_{obs} on the nucleotide concentration. (A) 1 μM WT MV 1IQ was mixed with varying concentrations of AMPPNP, and (B) 1 μM E442A MV 1IQ was mixed with varying ATP concentrations. Data points represent the average of 1−3 transients, and the solid lines are the best fits to a hyperbola. (Inset A: Time course of fluorescence enhancement after mixing 1 μM MV 1IQ with 200 μM AMPPNP. Inset B: Time course of fluorescence enhancement after mixing 1 μM E442A MV 1IQ with 10 μM ATP. The solid lines represent the best fit to a single exponential with a rate of 3.5 ± 0.04 s^{-1} for inset A and 24.7 ± 0.5 s^{-1} for inset B.)

The tryptophan fluorescence increase of E442A MV 1IQ was used to measure the rate of ATP binding (K_1k_{+2} = 2.7 ± 0.6 μM^{-1} s^{-1}), which was similar to that of WT MV 1IQ (K_1k_{+2} = 1.4 ± 0.2 μM^{-1} s^{-1}) (Table 2). The nucleotide-dependence of the rate of tryptophan fluorescence enhancement was best fit to a hyperbola. However, the difficulty in obtaining data points at high ATP concentrations (≥800 μM), due to the lower amplitude of the tryptophan fluorescence signal with E442A MV 1IQ, does not allow us to completely rule out a linear fit of the data. The data fit to a hyperbola suggest that the formation of the hydrolysis-competent state, derived from the maximum rate of the tryptophan fluorescence signal ($k_{+3a} + k_{-3b}$ = 731 ± 128 s^{-1}) (Figure 3B and Table 2), was very similar to that of WT MV 1IQ (770 ± 16 s^{-1}) (*6*).

Population of the Weakly Bound States Monitored with Pyrene Actin Fluorescence. The fluorescence from pyrene actin is quenched upon formation of the strongly bound actomyosin complex and recovers upon formation of a weakly bound actomyosin complex. Formation of the weakly bound states of MV 1IQ induced by nucleotide binding occurs in two steps; a rapid binding of nucleotide to actomyosin (K_1'), followed by a slower isomerization (K_2') to the weakly bound conformation (see Scheme 3, where A* represents unquenched pyrene actin fluorescence).

Scheme 3

$$AM + ATP \overset{K_1'}{\leftrightarrow} AM(ATP) \underset{k_{-2}'}{\overset{k_{+2}'}{\leftrightarrow}} A^*M.ATP \overset{K_8}{\leftrightarrow} A^* + M.ATP \overset{K_{3a}}{\leftrightarrow} M^*.ATP$$

The initial slope of the curve is a measure of the rate of nucleotide binding to actomyosin ($K_1'k_{+2}'$). The maximum rate is a measure of the forward rate constant for the isomerization step (k_{+2}'), when $k_{+2}' \gg k_{-2}'$ or the equilibrium constants K_8' and K_{3a} are high enough to favor the forward reaction. The plots demonstrating the ATP-induced population of weakly bound actomyosin V 1IQ are shown in Figure 4, and the calculated rate and equilibrium constants are summarized in Table 2. The amplitude of the pyrene fluorescence transient induced by binding of saturating concentrations of ATPγS or AMPPNP to actomyosin V 1IQ was 100% recovered, indicating that $k_{+2}' \gg k_{-2}'$ and the binding of these nucleotides is essentially irreversible. Mixing ATPγS with pyrene actomyosin V 1IQ resulted in a fluorescence transient that was best fit by two exponentials, with a maximum rate of the slow and fast phases calculated to be ∼7 and ∼70 s^{-1}, respectively. The slow phase was thought to be due to the small amount of ADP contamination in the ATPγS prep that competitively inhibits the binding of ATPγS to actomyosin V. The rate of ATPγS binding to actomyosin V 1IQ ($K_1'k_{+2}'$= 0.16 ± 0.04 μM^{-1} s^{-1}) was 10-fold slower than that of ATP ($K_1'k_{+2}'$= 1.0 ± 0.1 μM^{-1} s^{-1}) and resulted in a 10-fold slower rate of formation of the weakly bound actomyosin complex (k_{+2}' = 66 ± 10 s^{-1}) compared to that induced by ATP binding (k_{+2}' = 899 ± 43s^{-1}), while the equilibrium constant for rapid ATPγS binding to actomyosin V 1IQ was 2-fold tighter than that for ATP ($1/K_1'$ = 400 ± 160 and 925 ± 109 μM, respectively) (Figure 4A and Table 2). The pyrene actin fluorescence transients induced by AMPPNP binding to actomyosin V 1IQ were also best fit by two exponentials, of which the slower phase was modeled as the ADP-inhibited rate, as suggested for ATPγS. The second-order rate constant for the AMPPNP-induced population of weakly bound actomyosin V 1IQ ($K_1'k_{+2}'$= 0.003 ± 0.0001μM^{-1} s^{-1}) and the maximum rate of formation of the weakly bound conformation (k_{+2}' = 0.8 s^{-1} ± 0.1 s^{-1}) were much slower than that with ATP, while the rapid rate of AMPPNP binding was 2−3-fold tighter ($1/K_1'$ = 248 ± 81 μM) (Figure 4B and Table 2).

The ATP-induced population of the weakly bound acto−E442A MV 1IQ was very different from acto−G440A MV 1IQ. The properties of the ATP-induced population of weakly bound acto−E442A MV 1IQ ($1/K_1'$ = 387 ± 40 μM, $K_1'k_{+2}'$= 2.3 ± 0.2 μM^{-1} s^{-1}; k_{+2}' = 874 ± 28 s^{-1}) were nearly identical to WT MV 1IQ (Figure 4D and Table 2). The amplitude of the pyrene fluorescence increase following ATP binding to acto−G440A MV 1IQ was 70−80% recovered, indicating that k_{+2}' is not ≫ k_{-2}', and thus ATP binding may be more reversible with this mutant. Therefore,

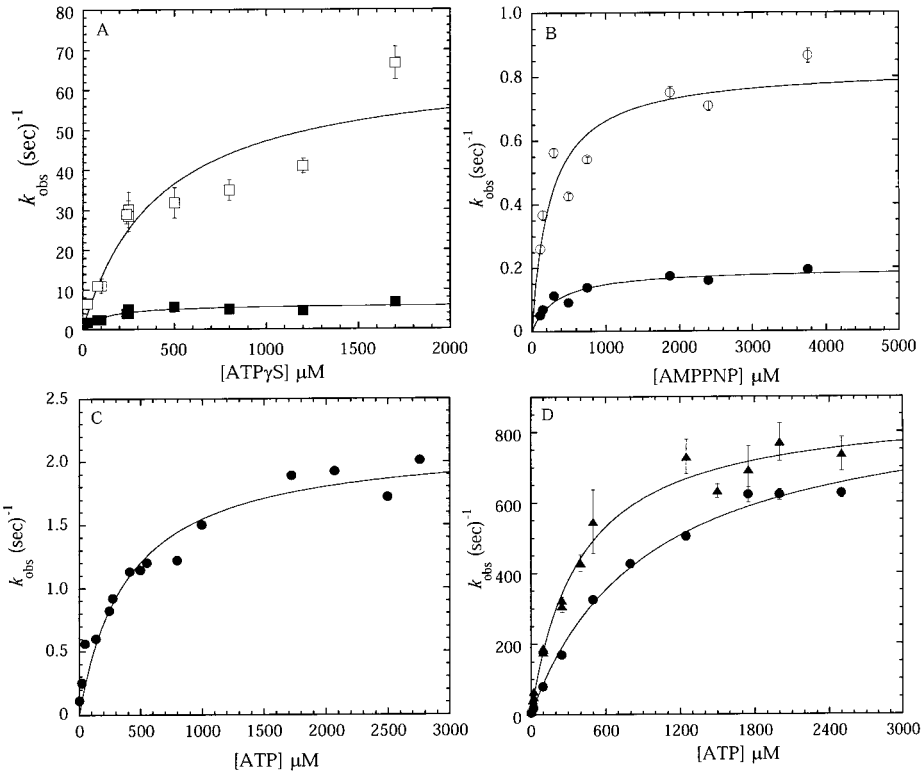

FIGURE 4: ATP- and ATP-analogue-induced population of weakly bound actomyosin V 1IQ monitored by pyrene actin fluorescence. Dependence of the rate of the fluorescence increase (k_{obs}) upon mixing 0.5 μM WT MV 1IQ bound to 0.5 μM pyrene actin and varying concentrations of ATPγS (A) or AMPPNP (B), as well as 0.5 μM MV G440A (C) or E442A (D) 1IQ bound to 0.5 μM pyrene actin mixed with varying ATP concentrations. The fluorescence increase in the presence of ATPγS or AMPPPNP was fit to two exponentials, and the fast phase was modeled to be the ATPγS or AMPPNP-induced dissociation (shown in A and B), while the slow-phase was modeled as the ADP-inhibited rate (maximum rate of $\sim$7 s^{-1} for ATPγS and $\sim$0.2 s^{-1} for AMPPNP). All other experiments were fit to single exponentials, and the error bars represent the standard error of the fit. The solid lines are best fits to a hyperbola. The data represent the summary of experiments from at least two separate protein and nucleotide-analogue preparations.

the rate and equilibrium constants describing the interaction of ATP and acto−G440A MV 1IQ are referred to as $K_1'k_{+2}'^{app}$ and $k_{+2}'^{app}$. Acto−G440A MV 1IQ had an equilibrium constant for rapid ATP binding that was 2−3-fold tighter ($1/K_1' = 398 \pm 71$ μM) than that for WT acto−MV 1IQ. In addition, acto−G440A MV 1IQ had a much slower second-order rate constant for ATP binding ($K_1'k_{+2}'^{app} = 0.005 \pm 0.001$ μM^{-1} s^{-1}), in contrast to that monitored by mantATP ($K_1'k_{+2}' = 1.2 \pm 0.1$ μM^{-1} s^{-1}), and populated the weakly bound states at a much slower rate ($k_{+2}'^{app} = 2.2 \pm 0.1$ s^{-1}) (Figure 4C and Table 2).

Affinity for Actin. The apparent affinity of MV 1IQ for actin (K_d^{app}) in the presence of nucleotide analogues or G440A and E442A MV 1IQ in the presence of ATP was determined using actin cosedimentation assays (Figure 5 and Table 2). The apparent affinity of MV 1IQ for actin in the presence of ATPγS was in the micromolar range ($K_d^{app} = 4.0 \pm 1.0$ μM and 13.0 ± 2.0 μM at 4 and 25 °C, respectively) after correcting the data for the amount of ADP bound to actomyosin V 1IQ ($\sim$20% at 4 °C and $\sim$80% at 25 °C) (Figure 4A). MV 1IQ had a much higher affinity for actin in the presence of AMPPNP ($K_d^{app} = 0.30 \pm 0.03$ μM) that was independent of temperature (Figure 4A). The E442A MV 1IQ was determined to have an affinity for actin in the micromolar range ($K_d^{app} = 1.6 \pm 0.2$ μM) in the presence of ATP at 25 °C, while G440A MV 1IQ had a $\sim$10-fold higher affinity for actin ($K_d^{app} = 0.20 \pm 0.02$ μM). In addition, the amplitude of the ATP-induced dissociation of acto−G440A MV 1IQ, which decreased as a function of pyrene actin concentration, was used to determine the affinity of the G440A MV1IQ mutant for pyrene actin in the presence of ATP ($\sim$0.6 μM) (data not shown).

DISCUSSION

The ability of myosin V to move processively along actin filaments requires that myosin V does not diffuse away from actin during multiple catalytic cycles. We have studied the weakly bound states of myosin V and ascertained that these states have a higher affinity for actin compared to the nonprocessive class II myosins and thus may contribute to myosin V's ability to move processively. Our results also have revealed a number of states that are involved in the communication between the nucleotide-binding pocket and the actin interface, and thus ATP-induced dissociation of actomyosin.

Tryptophan Fluorescence of Myosin V Monitors the Formation of the Hydrolysis-Competent State. The tryptophan fluorescence results with the nucleotide analogues and switch II mutants can be interpreted in terms of Scheme 4, modified from the scheme of myosin II (*25*, *26*), where M* represents enhanced myosin tryptophan fluorescence.

Since myosin V contains the conserved nucleotide-sensitive tryptophan residue (Trp-510 in skeletal muscle myosin II), it was proposed that the typtophan fluorscence increase probably monitors formation of the hydrolysis-competent step as has been shown in myosin II (*28*, *29*) or the transition from an open to a closed conformation (*11*).

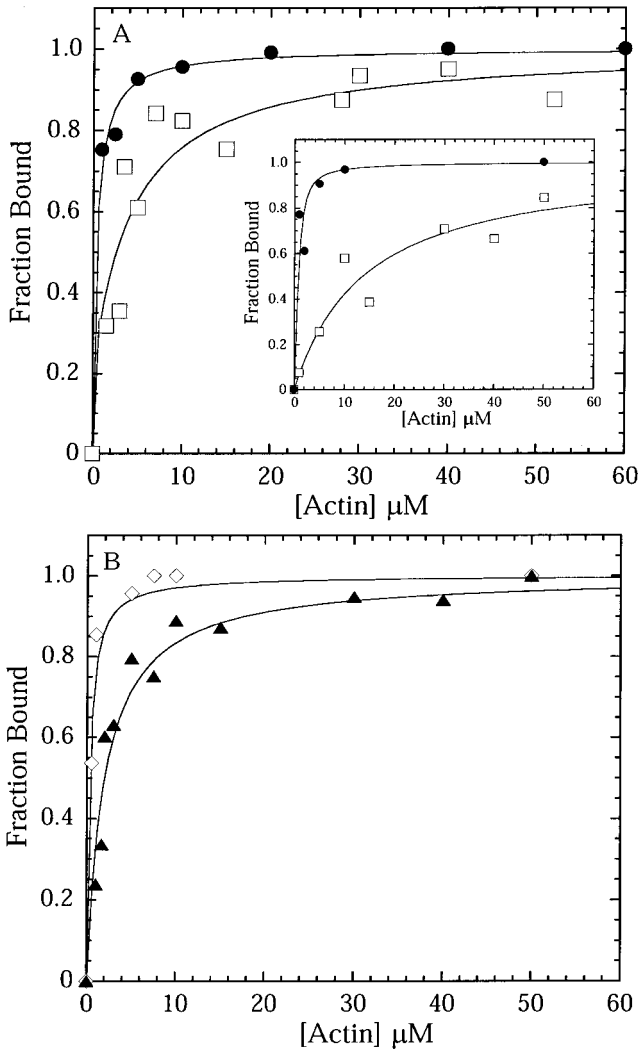

FIGURE 5: Apparent affinity for actin of MV 1IQ nucleotide complexes. Actin cosedimentation assay of MV 1IQ (1 μM) in the presence of (A) ATPγS (3 mM) (□) or (B) AMPPNP (5 mM) (●) at 4 °C (inset) or 25 °C. (B) MV G440A (1 μM) (◇) or E442A (1 μM) (▲) 1IQ in the presence of ATP (1 mM) at 25 °C. The amount of actin-bound myosin was determined by measuring the amount of MV 1IQ in the supernatant and pellet using Coomassie stained SDS-gels or HPLC analysis (see Materials and Methods). The data were corrected for the amount of AM(ADP) by using the competitive binding equilibrium equation (see Materials and Methods). The dissociation constant was determined by fitting the data to the quadratic equation (see Materials and Methods). The data represent the summary of experiments from at least two separate protein preparations.

Scheme 4

$$\underset{}{\overset{}{}} \quad \overset{\text{Open}}{} \quad \overset{\text{Closed}}{} \quad \overset{\text{Closed}}{}$$
$$\text{M} + \text{ATP} \leftrightarrow \text{M(ATP)} \leftrightarrow \text{M.ATP} \leftrightarrow \text{M*.ATP} \leftrightarrow \text{M*ADP.Pi} \leftrightarrow \text{M.ADP} \leftrightarrow \text{AM}$$

Therefore, in the presence of ATP, myosin V predominantly populates the M*.ADP.Pi state. Our data suggest that, as for myosin II, there are two different prehydrolysis ATP states in myosin V: a low-tryptophan fluorescence state (M.ATP or open) not capable of hydrolysis and a high-tryptophan fluorescence state capable of hydrolyzing ATP (M*.ATP or closed). Overall, our results support observations that formation of the hydrolysis-competent or closed state, which limits the rate of ATP hydrolysis, is extremely rapid (~700 s^{-1}) in MV 1IQ (*5*).

The intrinsic myosin V fluorescence experiments with nucleotide analogues suggest that they can effect formation and/or stabilization of the closed state. The intrinsic tryptophan fluorescence of MV 1IQ does not change in the presence of ATPγS even though MV 1IQ binds ATPγS rapidly and is capable of hydrolyzing this nucleotide analogue. ATPγS may slow the formation of the M*.ATP state in MV 1IQ, proceed through the M*.ATP to the M*.ADP.Pi state rapidly, and rapidly leave the M*.ADP.Pi state, preventing its accumulation. In addition, the hydrolysis of ATPγS by MV 1IQ is highly temperature-dependent and suggests myosin V mainly populates the M.ATP state at lower temperature. AMPPNP can induce a tryptophan fluorescence increase in MV 1IQ, despite its inability to hydrolyze AMPPNP. However, the amplitude of the fluorescence enhancement was ~50% of the enhancement observed with MV 1IQ in the presence of ATP, and the maximum rate of formation of the hydrolysis-competent or closed state was 200-fold slower than that of MV 1IQ. Since the rate of mantAMPPNP binding was determined to be faster ($\geq$~12 s^{-1}) than the maximum rate of tryptophan fluorescence enhancement, the data suggest that AMPPNP binds to MV 1IQ, followed by a slower rate of formation of the hydrolysis-competent state ($k_{+3a} + k_{-3b}$). Thus, AMPPNP binding to MV 1IQ induces formation of the closed state at a much slower rate than that of ATP, may reduce the equilibrium constant between the open and closed states, and results in population of a mixture of the M.ATP and M*.ATP states in the absence of actin.

The switch II mutants also trap myosin V in two different M.ATP states, suggesting a conserved structural mechanism for formation and stabilization of the closed state. The G440A MV 1IQ mutant binds ATP in a manner similar to WT MV 1IQ but does not populate the closed state, as indicated by the absence of an ATP-induced tryptophan fluorescence change. The intrinsic fluorescence signal of the E442A myosin V increased in the presence of ATP with an amplitude that was ~50% of WT MV 1IQ in the presence of ATP, while the kinetics of the tryptophan fluorescence enhancement of E442A MV 1IQ were similar to those of WT MV 1IQ. Sutoh and colleagues demonstrated that the corresponding mutations in *Dictyostelium* myosin II yielded similar results (*18*). In addition, the corresponding salt-bridge mutation in smooth muscle myosin II gave a similar result (*19*), but altering the charge at this position in Dicty myosin II prevented formation of the closed state (*17*). Therefore, the conserved switch II glycine, which forms a hydrogen bond to the γ phosphate, appears to be absolutely essential to drive rotation of the switch II helix and formation of the closed conformation. In addition, our data suggest that the conserved salt bridge between the switch I and II regions is not essential for formation of the closed conformation but may affect the equilibrium between the open and closed conformations.

Affinity for Actin in the Weak Binding States. The experiments performed in the presence of actin can be summarized in the following scheme (Scheme 5), in which ATP* represents enhanced mantATP fluorescence, M* represents enhanced myosin tryptophan fluorescence, and A* represents unquenched pyrene actin fluorescence. Scheme 5 demonstrates which state(s) we propose, WT or mutant MV 1IQ, mainly populate(s) in the presence of actin and

Scheme 5

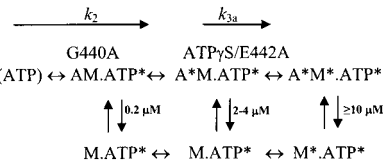

saturating nucleotide analogue or ATP concentrations, respectively. The two methods that were used to monitor the affinity of MV 1IQ for actin, pyrene actin fluorescence and actin cosedimnetation, allowed us to identify a state that is bound to actin, weakly tethered, but does not quench the pyrene actin fluorescence.

Previous results suggest ATP binding to actomyosin V 1IQ results in a rapid isomerization to a weak binding state that promotes dissociation from actin (*5*, *8*). Actin cosedimentation and pyrene actin dissociation data suggest that ATPγS induces a weakly bound state (K_d = 4 μM) that dissociates actomyosin V 1IQ. Also, the steady-state turnover of ATPγS by MV 1IQ is inhibited by actin with a concentration dependence that is similar to the affinity for actin measured by cosedimentation assays. The E442A MV 1IQ mutant in the presence of ATP, which is trapped in a mixture of the M.ATP and M*ATP states in the absence of actin, had a similar affinity for actin ($\sim$2 μM), suggesting this mutant may populate primarily the A*M.ATP* state in the presence of actin. In addition, previous experiments have determined that the affinity of the A*M*.ATP* state, which is the same structural state as the A*M*.ADP.Pi state, has a weak affinity for actin ($\geq$10 μM) (*5*). Interestingly, MV 1IQ's affinity for actin in the M.ATP-state at 50 mM KCl is much tighter than that of class II myosins ($\geq$30 μM) (*13*−*15*), suggesting that the actin binding region of myosin V is different from that of nonprocessive class II myosins. Since the binding of myosin to actin in the weak binding states is thought to be mediated by a charged loop (loop 2) (*30*, *31*), unresolved by crystallographic studies, the additional charged residues in or around this loop may contribute to myosin V's increased affinity for actin in the weak binding states as suggested (*8*).

The pyrene fluorescence of actomyosin V 1IQ fully recovers in the presence of AMPPNP indicating this ATP analogue can induce a state that does not quench pyrene, while its affinity for actin remains relatively high ($\sim$0.3 μM). The tryptophan fluorescence results with AMPPNP suggest this analogue can induce formation of the closed state (M*.ATP) in the absence of actin, but actin binding may cause the MV 1IQ.AMPPNP complex to shift to a state intermediate between weak and strong binding. Experiments with AMPPNP and muscle myosin II also suggest that AMPPNP can induce a state that has a higher affinity for actin than that in the presence of ATP or ATPγS (*13*). In addition, AMPPNP can induce activation of the thin filament in muscle (*32*) and results in cross-bridges that are immobile and stereospecifically bound to actin (*33*). Actomyosin V 1IQ in the presence of AMPPNP does not represent the same state as the acto−G440A MV 1IQ mutant in the presence of ATP even though they have similar affinities for actin, because the G440A MV 1IQ mutant quenches pyrene actin. Therefore, it is unclear what state actomyosin V 1IQ represents in the presence of AMPPNP, but it could represent a posthydrolysis M.ADP.Pi state such as that proposed by Sleep and Hutton (*34*) as well as Taylor (*35*), or a state off the normal ATPase pathway of myosin V.

The G440A MV 1IQ mutant traps myosin V in an M.ATP-state that has a relatively high affinity for actin ($\sim$0.2 μM) and ATP, suggesting this mutant uncouples the actin and nucleotide binding sites. The tryptophan fluorescence of G440A MV 1IQ mutant did not increase in the presence of ATP even though it bound ATP with a similar affinity to WT MV 1IQ in the presence and absence of actin (Table 2). The high affinity of the G440A MV 1IQ mutant for actin and its ability to quench pyrene actin fluorescence in the presence of ATP suggests this mutant occupies a state intermediate between weak and strong binding (AM.ATP*). Studies on myosin II suggest that a higher affinity for nucleotide would result in a lower affinity for actin (*36*). The results of the G440A MV 1IQ mutant bound to ATP suggest myosin V may be capable of adopting a state that can bind actin and ATP with moderate affinities. If this state is a normal part of the actomyosin V pathway, it is not significantly populated because the ATP-induced dissociation of actomyosin V is extremely rapid ($\sim$1000 s^{-1}).

The results with the G440A MV 1IQ mutant also demonstrate that the mantATP and pyrene actin fluorescence signals report two different structural transitions during the actomyosin ATP cycle (see Scheme 5). These results suggest that two different conformational changes occur when ATP binds actomyosin; first the nucleotide binding region changes conformation to bind ATP tightly, which alters the environment of the mant fluorophore (AM.ATP*), then there is an isomerization from a strong to a weak actomyosin complex (A*M.ATP*), which alters the environment of the pyrene fluorophore. The G440A mutant separates these two signals, which were previously thought to occur in the same step. Both steps occur rapidly in WT MV 1IQ and myosin II and therefore cannot be resolved.

ATP-Induced Dissociation of Actomyosin. Coordination of the γ phosphate of ATP is critical to induce the weakly bound actomyosin complex. Previous results suggest that the switch II region communicates conformational changes at the nucleotide binding site to the light chain binding region (*11*). Our results suggest that altering interactions with the γ phosphate, either by using a nucleotide analogue or by mutating a residue (G440A) involved in binding the γ phosphate, decreases the isomerization rate (k_{+2}') from strong to weak binding. Thus, conformational changes in the switch II region may also be coupled to changes in the actin-binding region.

The rate of this isomerization is quite fast in WT MV 1IQ in the presence of ATP ($k_{+2}' \sim 1000$ s^{-1}) and was reduced $\sim$1000-fold with AMPPNP ($k_{+2}'^{app} \sim 0.8$ s^{-1}), $\sim$500-fold in the G440A mutant ($k_{+2}'^{app} \sim 2$ s^{-1}), and $\sim$10-fold with ATPγS ($k_{+2}' \sim 70$ s^{-1}). The nucleotide-analogue-induced isomerization from strong to weak binding was also found to be reduced in skeletal muscle myosin II (*14*), which suggests that the structural interactions of the nucleotide in the active site of myosin are well conserved between class II and V myosins.

Crystallographic studies with myosin II suggest that AMPPNP and ATPγS are coordinated in the active site of myosin similarly to ATP, with a few specific differences that may be responsible for the different biochemical

properties observed with these two nucleotide analogues (*37*). The structure of AMPPNP bound to myosin displays a different hydrogen bonding pattern around the nucleotide than that of ATP, which likely reduces its affinity for myosin and slows the formation of a weak binding conformation in the presence of actin. In the case of ATPγS, the only difference is the sulfur atom, which replaces one of the oxygen atoms of the γ phosphate of ATP, disrupts hydrogen bonds that normally form with solvent molecules. Thus, very subtle structural difference between ATP analogues and ATP can have a dramatic effect on the hydrolysis step and formation of the weak binding conformation.

In the G440A MV 1IQ mutant, removal of the hydrogen bond between glycine 440 and the γ phosphate of ATP may eliminate rearrangements of the switch II region and prevent formation of the closed state (*18*). Our results add to the previous results by suggesting conformational changes in the switch II region are essential for forming the weak binding conformation, which may involve opening of the actin-binding cleft (*38*, *39*). This suggests that strong actin binding may alter the conformation of the switch II region and that ATP binding to actomyosin changes the conformation of the switch II region, which is necessary for forming a weakly bound conformation of myosin.

Implications for Processivity of the Native Myosin V Dimer. One model (*2*, *23*) proposes that a relatively high affinity for actin in the M.ADP.Pi state is important for the mechanism of myosin V or myosin VI processivity. This model suggests that the probability of entry into the strong actin binding states is a product of the two equilibrium constants, M.ADP.Pi binding to actin ($1/K_9$) and phosphate release (K_4'), which determines the degree of processivity of myosin V. Furthermore, it was proposed that after initially binding to actin in the M.ADP.Pi state, actin may induce formation of a state that precedes phosphate release and has an actin affinity that is intermediate between weak and strong (*23*). Since the M.ATP state has a relatively high affinity for actin, the affinity of the M.ADP.Pi state for actin may also be relatively high compared to nonprocessive myosin II. In addition, our results with AMPPNP show that myosin V is capable of forming a state that is intermediate between weak and strong actin binding. Therefore, a relatively high affinity for actin in the M.ADP.Pi state and extremely fast and irreversible phosphate release could both be important for the processivity of myosin V.

In conclusion, our results show that myosin V has a higher affinity for actin than muscle myosin II in the weak binding states. Our results suggest that specific interactions between ATP and myosin are extremely important for generating a weak binding conformation and promoting dissociation from actin. We provide direct evidence that during the ATP-induced dissociation of actomyosin the nucleotide binding region of myosin changes conformation, which is then transmitted to create changes in the actin-binding region. Specific mutations and analogues can partially uncouple the communication between the two sites. This draws further attention to the likelihood that high-resolution structures of the actin−myosin complex will reveal different conformations of the active site elements and the elements connecting them to the actin interface than have been seen in the myosin structures solved thus far.

ACKNOWLEDGMENT

The authors sincerely thank the anonymous reviewers for their critical comments on the manuscript and for suggesting the mantAMPPNP experiment. The authors also acknowledge the excellent technical assistance of Corry Baldacchino.

REFERENCES

1. Mehta, A. D., Rief, M., Spudich, J. A., Mooseker, M. S., and Cheney, R. E. (1999) *Nature 400*, 590−593.
2. Rief, M., Rock, R. S., Mehta, A. D., Mooseker, M. S., Cheney, R. E., and Spudich, J. A. (2000) *Proc. Natl. Acad. Sci. U.S.A. 97*, 9482−9486.
3. Sakamoto, T., Amitani, I., Yokota, E., and Ando, T. (2000) *Biochem. Biophys. Res. Commun. 272*, 586−590.
4. Nascimento, A. A. C., Chenay, R. E., Tauhata, S. B. F., Larson, R. E., and Mooseker, M. S. *J. Biol. Chem. 271*, 17561−17569.
5. De La Cruz, E. M., Wells, A. L., Rosenfeld, S. S., Ostap, E. M., and Sweeney, H. L. (1999) *Proc. Natl. Acad. Sci. U.S.A. 96*, 13726−13731.
6. De La Cruz, E. M., Wells, A. L., Sweeney, H. L, and Ostap, E. M. (2000a) *Biochemistry 39*, 14196−14202.
7. De La Cruz, E. M., Sweeney, H. L., and Ostap, E. M. (2000b) *Biophys. J. 79*, 1524−1529.
8. Trybus, K. M., Krementsova, E., and Freyzon, Y. (1999) *J. Biol. Chem. 274*, 27448−27456.
9. Wang, F., Chen, L., Arcucci, O., Harvey, E. V., Bowers, B., Xu, Y., Hammer, J. A., III., and Seller, J. R. (2000) *J. Biol. Chem. 275*, 4329−4335.
10. Vale, R. D. (1996) *J. Cell Biol. 135*, 291−302.
11. Geeves, M. A., and Holmes, K. C. (1999) *Annu. Rev Biochem. 68*, 687−728.
12. Gulick, A. M., Bauer, C. B., Thoden, J. B., and Rayment, I. (1997) *Biochemistry 36*, 11619−11628.
13. Berger, C. L., and Thomas, D. D. (1991) *Biochemistry 30*, 11036−11045.
14. Konrad, M., and Goody, R. S. (1982) *Eur. J. Biochem. 128*, 547−555.
15. Resetar, A. M., and Chalovich, J. M. (1995) *Biochemistry 34*, 16039−16045.
16. Friedman, A. L., Geeves, M. A., Manstein, D. J., and Spudich, J. A. (1998) *Biochemistry 37*, 9679−9687.
17. Furch, M., Fujita-Becker, S., Geeves, M. A., Holmes, K. C., and Manstein, D. J. (1999) *J. Mol. Biol. 290*, 797−809.
18. Sasaki, N., Shimada, T., and Sutoh, K. (1998) *J. Biol. Chem. 273*, 20334−20340.
19. Onishi, H., Kojima, S., Katoh, K., Fujiwara, K., Martinez, H. M., and Morales, M. F. (1998) *Proc. Natl. Acad. Sci. U.S.A. 95*, 6653−6658.
20. Hiratsuka, T. (1983) *Biochim. Biophys. Acta 742*, 496−508.
21. Pardee, J. D., and Spudich, J. A. (1982) *Methods Enzmol. 85*, 164−181.
22. Pollard, T. D. (1984) *J. Cell Biol. 99*, 769−777.
23. De La Cruz, E. M., Ostap, E. M., and Sweeney, H. L. (2001) *J. Biol. Chem. 276*, 32373−32381.
24. Geeves, M. A., and Jeffries, T. E. (1988) *Biochem. J. 256*, 41−46.
25. Bagshaw, C. R., Eccleston, J. F., Eckstein, F., Goody, R. S., Gutfreund, H., Trantham, D. R. (1974) *Biochem J. 141*, 351−364.
26. Johnson, K. A., and Taylor, E. W. (1978) *Biochemistry 17*, 3432−3442.
27. De La Cruz, E. M., and Pollard, T. D. (1996) *Biochemistry 35*, 14054−14061.
28. Yengo, C. M., Chrin L. R., Rovner, A. S., and Berger, C. L. (2000) *J. Biol. Chem. 18*, 25481−25487.
29. Malnasi-Csizmadia, A., Woolley, R. J., and Bagshaw, C. R. (2000) *Biochemistry 39*, 16135−16146.
30. Mornet, D., Bertrand, R. U., Pantel, P., Audemard, E., and Kassab, R. (1981) *Biochemistry 21*, 2110−2120.
31. Sutoh, K. (1982) *Biochemitry 21*, 2110−2120.

32. Greene, L. (1982) *J. Biol. Chem. 257*, 13993−13999.
33. Fajer, P. G., Fajer, E. A., Brunsvold, N. J., and Thomas, D. D. (1988) *Biophys. J. 53*, 513−524.
34. Sleep, J. A., and Hutton, R. L. (1980) *Biochemistry 19*, 1276−1283.
35. Taylor, E. W. (1991) *J. Biol. Chem. 266*, 294−302.
36. Geeves, M. A., Jeffries, T. E., and Millar, N. C. (1986) *Biochemistry 25*, 8454−8458.
37. Bauer, C. B., Holden, H. M., Thoden, J. B., Smith, R., and Rayment, I. (2000) *J. Biol. Chem. 275*, 38494−38499.
38. Yengo, C. M., Gaffney, D. M., Chrin, L. R., and Berger, C. L. (2001) *Biophys. J. 80*, 198a.
39. Volkmann, N., Hanin, D., Ouyang, G., Trybus, K. M., DeRosier, D. J., and Lowey, S. (2000) *Nat. Struct. Biol. 7*, 1147−1155.

BI015969U